

Vortex Formation in the Wake of Dark Matter Propulsion

G. A. Robertson¹ and M. J. Pinheiro²

¹*Institute for Advanced Studies in the Space, Propulsion & Energy Sciences
265 Ita Ann, Madison, AL 35757
256-694-7941; gar@ias-spes.org*

²*Department of Physics & Institute of Plasma and Nuclear Fusion
Instituto Superior Tecnico, Av. Rovisco Pais
1049-001 Lisboa, Portugal
mpinheiro@ist.utl.pt*

Abstract. There is a general view that closed currents pervade the entire universe and, in particular, there is a cosmic mechanism to expel matter to large astronomical distances involving vortex currents as seen with blazars and blackholes. At the terrestrial level force producing vortices have been related to the motion of wings (*e.g.*, birds, duck paddles, fish's tail). In this paper, vortex structures are shown to exist aft of a spaceship using the density excitation method per the modified Chameleon model. This vortex structure is then shown to have similarities to spacetime models as Warp-Drive and wormholes, giving rise to the natural extension of Hawking and Unruh radiation, which provides the propulsive method for space travel where *virtual electron-positron pairs*, absorbed by the gravitational expansion forward of the spaceship emerge from an annular vortex field aft of the spaceship *as real particles*, in-like to propellant mass ejection in conventional rocket theory.

Keywords: Electromagnetism, Optics, Acoustics, Heat Transfer, Classical Mechanics, And Fluid Dynamics, Other Topics In General Theory Of Fields And Particles, Electromagnetic Processes And Properties, Electrokinetic Effects, Magnetohydrodynamics And Electrohydrodynamics

Pacs: 40., 11.90.+t, 13.40.-f, 47.57.jd, 47.65.-d

INTRODUCTION

In a recent paper (Pinheiro, 2010), the second author introduce the concept of electromagnetotoroid in astrophysics and its role in polar jets, showing that it represents the onset of Abraham's force driven by some external source. He further showed that the Abraham's force term is the analogue of the Magnus force, and thus represents the formation of vortex structures, of electromagnetic nature, in the fabric of space-time. This was shown to prove that major natural propulsion processes on Earth (*e.g.*, birds, fishes) and in the Universe (*e.g.*, Herbig-Haro objects as seen with blazars and blackholes) all have the same underlying nature at their base.

Over the last few years, the first author (Robertson, 2009a, 2009b and 2010) introduced a modified Chameleon model for use in propulsion derived from the Khoury and Weltman Chameleon Theory (2004a and 2004b). The Chameleon theory is a dark matter/energy theory that assumes forces from the change in densities in or about an object. In this paper, it will be shown that at high accelerations to near light speeds, the modified Chameleon model produces a vortex structure aft of a moving object in the Chameleon (dark matter/energy) field that has similarities to spacetime models as Warp-Drive and Wormholes.

Further, it will also be shown that the Chameleon vortex propulsion model is a natural extension of the interaction between Hawking and Unruh radiation, which provides a new roadmap toward new innovative space propulsion systems that are founded in both nature and theory.

VORTEX CURRENT STRUCTURES IN NATURE

Birkeland (1903; Carlqvist 1988) proposed that magnetic disturbances accompanying the aurora boreal were caused by large electric currents flowing along the contours of the auroral zone, and Birkeland suggested that the current entered from one end and left at the other, in a complete closed circuit. Although at the time the idea was not well accepted, in 1973 the Triad satellite have shown conclusively that the large-scale pattern of such (closed) currents do exist (Potemra, 1978).

Different but related phenomena are the Herbig-Haro (HH) objects observed by Burnham (1890). HH objects are highly collimated, highly ionized matter ejections, which in the second author's viewpoint are propelled by a similar mechanism as presented above. For example, stars in their first hundred thousand years of existence are often surrounded by accretion disks build-up by gas (plasma, or just a good conductor) falling onto the black hole attracted by the strong gravitational field. The accretion disk is formed most probably because there is an oblate spheroid attracting particles. When particles fall into the center angular momentum flow outwardly, the proposed mechanism is MHD turbulence (Priest, 2000) as the accretion disks are not devoid of magnetic fields, and since they constitute a current of ionized particles falling into a black hole.

Kronenberg *et al.* (2001) suggested that magnetic field lines (produced from closed astrological currents) extend a few million light years from galaxies into the intergalactic medium. Although the mechanism is not fully understood, the black hole accretion disk energy could be converted into magnetic fields through the agency of efficient energy-producing dynamos within black holes, a kind of cosmic electric motor. Occasionally black holes eject huge amounts of gas. In particular, blazars might expel jets of plasma into space, a phenomena observed by a team from the blazar *BL Lacertae*, the plasma jet spiraling outward from the flattened disk of spinning gas surrounding the supermassive black hole (Figure. 1) extending 950 million light years beyond (Marscher *et al.*, 2008).

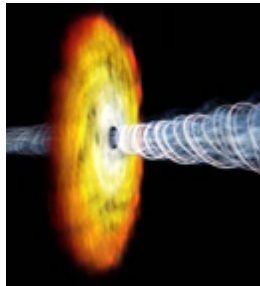


Figure 1. An artist concept of a spiraling (vortex) jet of high-energy particles (plasma) shooting out of the polar region of a supermassive black hole of a distant galaxy.

Newly forming (“pre-T-Tauri”) stars are usually surrounded by bipolar jets and molecular outflows in regions with small patches of nebulosity associated with newly born stars (*i.e.*, Herbig-Haro objects). Several models have been proposed to explain jet ejection-accretion processes and it is becoming evident that pure hydrodynamical models are not sufficient, and most probably MHD magneto-centrifugal ejection seems at the source of the driving mechanism (Cabrit, 2007). Optical observations (Hartigan, Edwards and Pierson, 2004) indicates that jets are produced in regions 5.5 AU in diameter, while attaining distances 800 AU in length and widths with Mach angles typical for free lateral expansion of a supersonic jet.

These references concur to the general view that closed currents pervade the entire universe and, in particular, there is a cosmic mechanism to expel matter to large astronomical distances involving vortex currents with similarities to the vortex shown in Figure 1. Therefore, one should suspect other similarities in nature at the terrestrial level involving force producing vortices. In fact, Dickinson (2003), with further discussion by the second author (Pinheiro, 2010), has shown that the main propulsion mechanism in nature relies on the production of vortices for some material structures (*e.g.*, wing, duck paddles, fish's tail) as shown in Figure 2. That is, fishes swim by flapping their tail and other fins, and squid and salps, eject fluid intermittently as a jet, producing optimal vortex rings which give the maximum thrust for a given energy input (Linden and Turner, 2004). Also, quite interestingly, their trajectory is done by crossing the vortex produced at each stroke, like traveling through a channel of vortices.



Figure 2. Locomotion in fluids and vortical structure generated at each stroke by bird and fish (Pinheiro, 2010).

THE CHAMELEON MODEL

The Chameleon Theory (Khoury and Weltman, 2004a and 2004b) represents a fifth force of nature. This fifth force is given as a Chameleon (*i.e.*, hiding within known physics) scalar field tied to the density of matter through a thin-shell concept or mechanism. Such an analogy gives the Chameleon field dark energy/dark matter like characteristics (see: Brax *et al.*, 2004a and 2004b; Robertson, 2010); fitting well within the cosmological expansion (see: Robertson, 2009a) and provides a mechanism to carry currents throughout the Universe. The foundation of the thin-shell mechanism was developed by concentrating on the static solution where time fluctuations are set to zero within and about a spherically symmetric and significantly large object of homogeneous density ρ_m , mass m and radius R_m having a thin shell thickness ΔR_m . The thin shell model is illustrated in Figure 3, where the thin-shell thickness $\Delta R_m \ll R_m$ and is shown large in the figures for clarity.

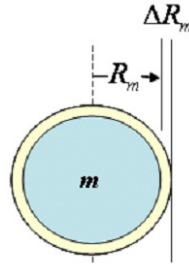


FIGURE 3. Chameleon thin-shell model.

The first author (Robertson, 2009a) showed that the thin shell thickness can be given by

$$\Delta R_m \approx 1/3 \left(M_E^2 / R_m \hat{\beta}_C \rho_m \right) \left(2M_{PL}^4 / \rho_0 \right)^{1/3} \left(1 - (\rho_0 / \rho_m)^{1/3} \right), \quad (1)$$

where $M_E \approx 10^4 m^{-1}$ is the universe energy scale factor, $M_{PL} = 4.34 \times 10^{-9} kg$ is the reduced Planck mass, $\hat{\beta}_C$ is the motion coupling to the external Chameleon field, ρ_0 is the external surrounding mass density. Then letting the external density ρ_0 be constant and $\ll \rho_m$, the thin shell thickness becomes solely a function of $(\hat{\beta}_C R_m \rho_m)^{-1} = (4\pi R_m^2 / 3m) \hat{\beta}_C^{-1}$. For a constant mass with $\hat{\beta}_C \sim 1$ as done in the Chameleon Model, equation (1) indicates an object's thin shell will change as the square of its radius. That is, even for a constant mass, as the radius of an object gets smaller the thin shell gets smaller. For example, the thin shell of a sun with radius R_{sun} will be larger than the thin shell of a black-hole with the same mass, but having a radius $\ll R_{sun}$. Generally, this infers that as the density of an object increases, the thin shell decreases.

The Chameleon theory implies a correction to the gravitational force as $F = (1 + \theta)F_{N_m}$, where $F_{N_m} = mg_m$ is the standard force of gravity and θ is the fifth force coefficients. The fifth force F_m is given in terms of the thin shell thickness as

$$\vec{F}_m \approx \theta \vec{F}_{N_m} = 6\beta_m (\Delta R_m / R_m) \vec{F}_{N_m} \quad (2)$$

where β_m is the object's coupling factor to the external Chameleon field.

Equation (1) indicates that as the radius R_m of a constant mass decreases (*i.e.*, increasing its density ρ_m), so does its thin shell thickness. That is, high density objects have smaller thin shell thicknesses than less dense objects. However, for the thin shell to decrease, the object's coupling β_m to the external Chameleon field must increase. That is, the gravitational pull on the external Chameleon field increases with increases in the coupling β_m , which in effect gravitationally compresses the thin shell. (This fact is a key factor in the far-space propulsion model discussed later.)

However, this does not necessary mean that the fifth force F_m on an object changes. For decreases in the ratio $\Delta R_m / R_m$ can be offset by the increase in the coupling β_m .

The Modified (Acceleration) Chameleon Model

The Modified Chameleon Model (Robertson, 2009a, 2009b and 2010) is founded on the fact that time fluctuations can exist within and about an object, such that, densities can vary even if only slightly to cause changes in an object's internal or external Chameleon scalar field; affecting the thin shell thickness about an object. And that the changes in the density can be induced linearly in the direction of motion. Whereby, the thin-shell about an object will change accordingly. This is illustrated by an increase in the thin shell thickness in the direction of motion and a decrease in the thin shell opposite to the direction of motion. The increase in the thin shell thickness in the direction of motion is proportional to the square of the acceleration of the object and the decrease in the thin shell opposite to the direction of motion is proportional to one over the square of the acceleration of the object – this was ignored in the previous papers, but will be discussed further later in this paper.

External Chameleon Field Changes: Coupling Excitation Model

The modified Chameleon model represents small variations in the gravitational force as the gravitation field is an accelerated field. For example, the object of mass m in Figure 3 is accelerated toward a larger object of mass $M \gg m$. Here there is a continuous battle between the (internal and external) particulate matter of the smaller object caused by the interaction between the background Chameleon field and the larger object's internal Chameleon field, which produces a change $\partial \Delta R_m$ in the thin shell thickness as shown in Figure 4; predominately in the direction of the acceleration force (*i.e.*, gravity). That is, the thin shell is minimally coupled to gravity, but strongly coupled to the affects of the accelerated Chameleon field. In this model, any change to the density of the object is assumed to be small. (In the Modified Chameleon Model, the symbol ∂ infers a change and not a derivative.)

The sum of the fifth force $\sum \theta \cdot F_{N_M}$ on the smaller object effects its (gravitational) acceleration force according to $F = (1 + \sum \theta)F_{N_M}$, where $F_{N_M} = mg_M$ and $\sum \theta$ is the sum of the fifth force coefficients about the smaller object. The fifth force F_m is given in terms of the thin shell thickness according to equation (2) as

$$F_m \approx \sum \theta F_N = 6\partial \beta_m (\partial \Delta R_m / R_m) F_{N_m} \quad (3)$$

where $\partial \beta_m$ is the change in the object's coupling factor to the external Chameleon field and where from equation (1) the change in the thin shell

$$\partial\Delta R_m \approx 1/3 \left(M_E^2 / R_m \partial\hat{\beta}_C \rho_m \right) \left(2M_{PL}^4 / \rho_0 \right)^{1/3}, \quad (4)$$

and we let $\partial\Delta R_m \gg \Delta R_m$ and $\rho_m \gg \rho_0$. Noting that the thin-shell change in equation (4) is due solely to the change in the motion coupling $\hat{\beta}_C$.

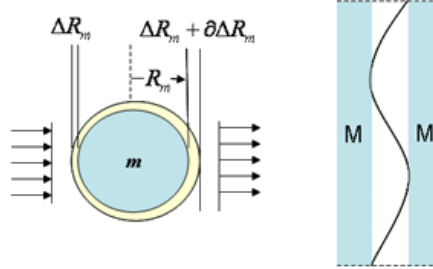


FIGURE 4. The Modified Chameleon Model.

During the development of this model, it was found that for the earth

$$\Delta R_m \approx \beta_m^2 \sqrt{l_p R_m}, \quad (5)$$

where $\beta_m \approx 1$ for a non-accelerated object, but implies that for an accelerated object that $\partial\Delta R_m \approx \partial\beta_m^2 \sqrt{l_p R_m}$, such that combining equations (4) and (5) yields

$$\partial\beta_m \approx \left(\left(\partial\hat{\beta}_C \sqrt{l_p R_m^3} \right)^{-1} 1/3 \left(M_E^2 / \rho_m \right) \left(2M_{PL}^4 / \rho_0 \right)^{1/3} \right)^{1/2}. \quad (6)$$

Example – For the earth, the modified and unmodified Chameleon models must give similar results. Then by combining equations (4) and (5) with $\partial\beta_\oplus \approx \partial\hat{\beta}_{C_\oplus} = 1$ yields

$$\sqrt{l_p R_\oplus} \approx 1/3 \left(M_E^2 / R_\oplus \rho_\oplus \right) \left(2M_{PL}^4 / \rho_{atm} \right)^{1/3},$$

where equation (6) is reduce to

$$\partial\beta_\oplus^2 \approx \left(\partial\hat{\beta}_{C_\oplus} \right)^{-1}.$$

That is, for the modified and unmodified Chameleon models to be the same, any change in the motion factor $\partial\hat{\beta}_{C_\oplus}$ is reflected on the mass coupling $\partial\beta_\oplus$.

- Of note, the earth example infers that when the object and the surrounding ambient field are both subject to the same acceleration, the motion factor $\partial\hat{\beta}_C \approx 1$.

Internal Chameleon Field Changes: Density Excitation Model

An important factor of the Modified Chameleon model is that an object's internal field density change $\partial\rho_m$ (noting this is not an actual matter density change) can produces a similar motion effect to that shown in Figure 4 without the presence of an external large mass, such that, equation (4) can be written as

$$\partial\Delta R_m \approx 1/3 \left(M_E^2 / \partial R_m \partial\hat{\beta}_C \partial\rho_m \right) \left(2M_{PL}^4 / \rho_0 \right)^{1/3}, \quad (7)$$

where the change in the motion factor $\partial\hat{\beta}_C$ arises from the change in the object's field density $\partial\rho_m$ with respect to the object's radial field change ∂R_m . Here, the acceleratory effect on the ambient field ρ_0 is due locally to the

object's acceleration of gravity g_m , where generally the object's acceleration $a_m > g_m$. That is, the object and ambient field are accelerating differently, such that, the motion coupling $\partial\hat{\beta}_c \neq 1$.

In this model, an object's field density change is due to the acceleration of the internal particulate matter of mass m_i , where the internal particulate matter never leaves the object, but relaxes back into the object over its normal relaxation time between impulses and infers a linear or directional phasing φ of the density. Typically, the phasing is relativistic, where the phase

$$\varphi \approx 1 - v_{relax}/c, \quad (8)$$

is used and where v_{relax} is the relaxation velocity of the accelerated particulate matter back into the object (Robertson, 2010). The forward object's mass coupling factor is given as

$$\partial\beta_{FW} \approx (a_m/g_m)/6\varphi \quad (9)$$

and the aft object's mass coupling factor

$$\partial\beta_{aft} = 1/\partial\beta_{FW}. \quad (10)$$

The object's field density change is given by

$$\partial\rho_m \approx \rho_m + (a_i/g_m)\rho_i = 3m/(4\pi \cdot \partial R_m^3), \quad (11)$$

where a_i is the acceleration of the internal particulate matter *in the direction of motion*, noting that the object's acceleration a_m and the internal particulate matter acceleration a_i are not necessarily equal.

- The author notes that the internal particulate matter needs to be coherent, which typically requires that internal particulate matter be no bigger than subatomic particles as atoms and larger matter become subject to large scale random collisions, which reduces the overall coherence – effecting the total density change in the object. Exclusion to this is the standard rocket model; see Robertson (2010), where large scale mass coherence occurs in the nozzle. Current examples of experimental devices that have produced excitation of internal particulates include: Brito, 2004; Feigel, 2004; Shawyer, 2008; Woodward, 2009 and 2010, which generally excite electron/photon motion within materials.

Equation (11) yields the object's changed field radial factor

$$\partial R_m = \left((1 + a_i/g_m (m_i/m))^{-1} \right)^{1/3} R_m. \quad (12)$$

The changed field radial factor ∂R implies that the object's internal Chameleon field density footprint decreases, not its actual matter radius.

The acceleration of the internal particulate matter *in the direction of motion* implies an energy change across the object that produces different changes in the thin-shells forward (FW) and aft of the object given from equation (4) as

$$\partial\Delta R_{FW} \approx 1/3 \left(M_E^2 / \left(\partial\hat{\beta}_{c_{FW}} \partial R_m \partial \rho_m \right) \right) \left(2M_{PL}^4 / \partial\rho_{FW} \right)^{1/3} \quad (13)$$

and

$$\partial\Delta R_{aft} \approx 1/3 \left(M_E^2 / \left(\partial\hat{\beta}_{c_{aft}} \partial R_m \partial \rho_m \right) \right) \left(2M_{PL}^4 / \partial\rho_{aft} \right)^{1/3}, \quad (14)$$

where $\partial\hat{\beta}_{c_{FW}}$ is the forward changed motion factor and $\partial\hat{\beta}_{c_{aft}}$ is the aft changed motion factor.

Then from equation (5), we let

$$\partial\Delta R_{FW} \approx \partial\beta_{FW}^2 \sqrt{I_p \partial R_m} \quad (15)$$

and

$$\partial\Delta R_{aft} \approx \partial\beta_{aft}^2 \sqrt{l_p \partial R_m} , \quad (16)$$

where equations (13) and (15) yields the forward Chameleon density factor

$$\partial\hat{\beta}_{C_{FW}} \approx 1/3(\partial\beta_{FW}^2)^{-1} \left(M_E^2 / \partial\rho_m \sqrt{l_p \partial R^3} \right) (2M_{PL}^4 / \rho_c)^{1/3} \quad (17)$$

and equations (14) and (16) yields the aft Chameleon density factor

$$\partial\hat{\beta}_{C_{aft}} \approx 1/3(\partial\beta_{aft}^2)^{-1} \left(M_E^2 / \partial\rho_m \sqrt{l_p \partial R^3} \right) (2M_{PL}^4 / \rho_c)^{1/3} \approx \partial\hat{\beta}_{C_{FW}} \partial\beta_{FW}^4 . \quad (18)$$

using, equations (10) and (17).

The Far-Space Propulsion Example

Consider a spaceship far from any large masses with mass $m_s = 10^4$ kg, effective radius $R_s = 10$ m and density $\rho_s \approx 2.387$ kg/m³. In far space with no mass density change, the spaceship is accelerating with the background (Universe) expansion, such that, the spaceship's motion coupling factor $\hat{\beta}_C = 1$. However, the field coupling factor, given from equations (14) as

$$\beta_s \approx \left(1/3 \left(M_E^2 / \hat{\beta}_C \rho_s \sqrt{l_p R_s^3} \right) (2M_{PL}^4 / \rho_c)^{1/3} \right)^{1/2} \quad (19)$$

which is $\sim 2.09 \times 10^{10}$. From equation (1) with $\rho_0 = \rho_c \ll \rho_s$, the spaceship's thin shell thickness $\Delta R \approx 5.567 \times 10^3$ m, noting that the same value is achieved using equation (5).

Now consider that the spaceship has the capability to modulating its density, or say just the propulsive mechanism, through the excitation of internal particulates of total mass $m_i = 10^{-4} m_s$. Since the particulate matter has the same effective radius as the spaceship, the particulate matter's density $\rho_i \approx 10^{-4} \rho_s$. Then given a particulate matter forward acceleration $a_i = c/2s$ and spaceship gravitational acceleration $g_s = G \cdot m_s / R_s^2 = (4\pi/3) R_s G \rho_s \approx 6.674 \times 10^{-9}$ m/s², the spaceship density change $\partial\rho_s \approx 5.362 \times 10^{12}$ kg/m³ from equation (11) and radial footprint change $\partial R \approx 7.636 \times 10^{-4}$ m from equation (12).

Now letting the particulate matter relaxation velocity $v_{relax} = \frac{1}{2}c$ gives the phase $\varphi = \frac{1}{2}$ from equation (8). So if the spaceship accelerates, say $a_s = 10^{-8} a_i \approx 1.5$ m/s², the spaceship forward field coupling factor change $\partial\beta_{FW} \approx 7.486 \times 10^7$ from equation (9). That is, the coupling to the Chameleon field forward the spaceship is $\sim 10^2$ times weaker than when the particulate matter is not accelerating. Noting the spaceship aft field coupling factor change $\partial\beta_{aft} \approx 1.336 \times 10^{-8}$ from equation (10), $\sim 10^{18}$ times weaker than when the particulate matter is not accelerating. Whereby, the differential field coupling across the spaceship is $\sim 10^{16}$ times greater in the forward direction.

Using these coupling factors and equations (15) and (16), the forward and aft thin shell changes are $\partial\Delta R_{FW} \approx 6.23 \times 10^{-4}$ m and $\partial\Delta R_{aft} \approx 1.982 \times 10^{-35}$ m. That is, although the thin shell is greatly compressed about the spaceship, the forward thin shell is still $\sim 10^{30}$ time greater than the aft thin shell. That is in respect to each other, the forward thin shell has a greater gravitational expansion than the aft thin shell, which is more gravitationally compressed.

Finally, from equations (17) and (18), the forward and aft motion coupling factor changes are $\partial\hat{\beta}_{FW} \approx 5.214 \times 10^{-2}$ and $\partial\hat{\beta}_{aft} \approx 1.638 \times 10^{30}$. Noting that the small value of the forward motion coupling factor indicates that an observer forward of the spaceship sees the spaceship accelerating toward the observer and the large value of the aft motion coupling factor indicates that an observer aft of the spaceship sees the spaceship accelerating away from the observer.

As a general note, the motion coupling factors behave like pressure indicators, *i.e.*, high pressure pushing on low pressure. On the other hand the field coupling factors are field attraction indicators, *i.e.*, high coupling – high attraction, low coupling – low attraction. Further, values of unity indication high gravitational attraction and near zero field attraction and pressure.

Light Speed Example

If the spaceship accelerates, say $a_s = a_i = \frac{1}{2}c$, the spaceship forward mass coupling factor change $\partial\beta_{FW} \approx 7.486 \times 10^{15}$ from equation (16). That is, the coupling to the Chameleon field forward the spaceship is $\sim 10^{15}$ times stronger than when the particulate matter is not accelerating. Noting the spaceship aft field coupling factor change $\partial\beta_{aft} = 1/\partial\beta_{FW} \approx 1.336 \times 10^{-16}$, $\sim 10^{-16}$ times weaker than when the particulate matter is not accelerating. Using these coupling factors and equations (12) and (13), the forward and aft thin shell changes are $\partial\Delta R_{FW} \approx 6.23 \times 10^{12} m$ and $\partial\Delta R_{aft} \approx 1.982 \times 10^{-51} m$.

A model of the gravitational expansion of the forward thin shell and the gravitational compression of the aft thin shell is shown in Figure 5. As shown, the gravitational expansion extends the forward thin shell in a conic fashion as it is connected to the spaceship, but the gravitational compression of the aft thin shell flattens the thin shell against the spaceship mass.

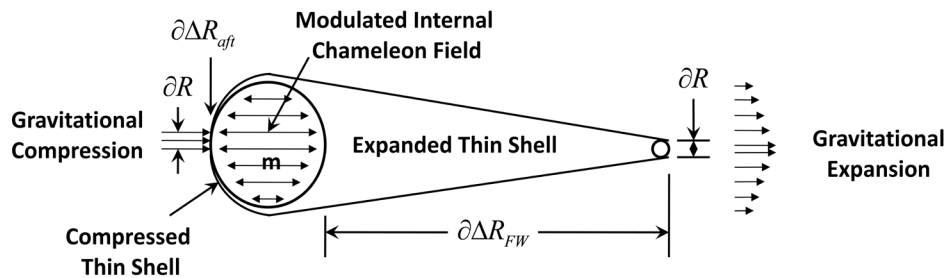


Figure 5. Gravitational Coupling of the External Chameleon Field Forward and Aft of a Spaceship of Mass m

VORTEX FORMATION IN THE WAKE OF THE CHAMELEON FIELD

Now placing the affects given in Figure 5 into the Universe Chameleon field as illustrated in Figure 6, it is found that a void exist aft of the spaceship above and below the radial area defined by ∂R . This is in line to the wake behind an object traveling through any fluid medium.

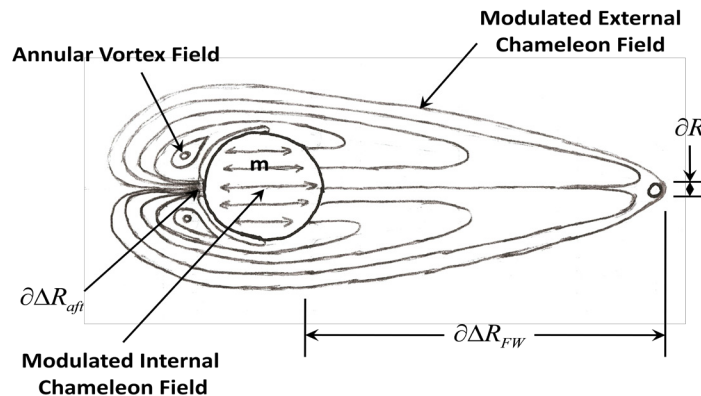


Figure 6. Spaceship of Mass m Traveling through the Universe Chameleon Field at Light Speed

From the standpoint of known physics, the motion of the spaceship must be somehow grounded to natural phenomena. In the wake aft of the spaceship mass (m_s) in Figure 6, the Chameleon field lines forms an annulus or vortical structure about the Chameleon field lines interring the reduced radial area defined by ∂R . Since the field lines about the annulus are closed, they represent the thin shell about virtual mass. By assuming that this virtual mass are electron like, one can then assume that there is an inward force on the annulus due a Chameleon Magnus effect that squeezes the Chameleon field lines interring the reduced radial area. This is the Chameleon field analogy to pinching in magnet-current phenomena (as in electromagnetically pinched plasma) and provides an action force on the aft thin shell of the spaceship in the direction of motion, which in turn implies a force on the forward thin shell in the direction of motion – *i.e.*, cause an effect.

Further, due to the curvature of the Chameleon field about the annulus the rotating annulus has an upward and aftward force exerted on it, which forces the annulus away from the spaceship mass, only to reform a new annulus as the older annulus moves away. This is the Chameleon field analogy to the locomotion in fluids by vertical structures generated at each stroke by a bird or fish as shown in Figure 2.

SIMILARITIES TO CONVENTIONAL PROPULSION

Similarities of the modified Chameleon model can be found in conventional propulsion. For example, similarities to conventional rocketry are shown in Figure 7 with respect to Figure 5. As shown, the accelerated exhaust between the nozzle and the shock diamond represent the modulated Chameleon field with the nozzle throat and shock diamond representing the gravitational expansion and compression. Whereby, the thin-shell expansion in the nozzle is the force mechanism. An annular Vortex field is not present as the velocity of the modulated Chameleon field is much-much less than light speed.

These similarities exist even though the mass flow from the rocket is opposite the particulate matter flow in the mass of Figure 5. This reversal is due to the matter in the mass flow being greater than subatomic particles, whereby the sign on the Chameleon field pressure is reversed while the other physical characteristics remain the same.

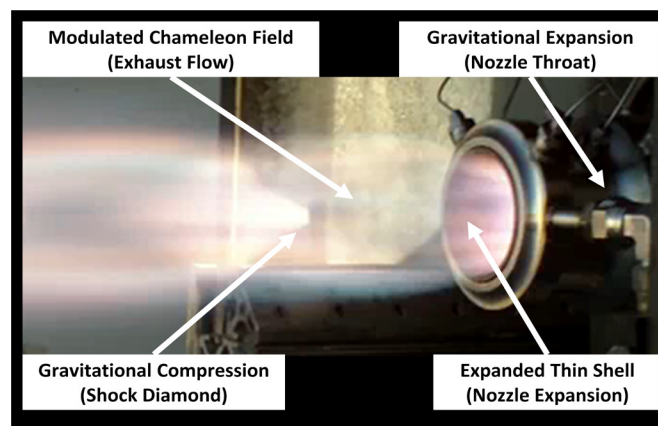


Figure 7. Similarities to Conventional Rocketry.

It is noted that the repetition of shock diamonds as seen in rocket exhausts would also be seen by an observer watching the flyby of a spaceship using the particulate mass changing density method of the modified Chameleon model. However, the radiation may not be visible to humans, but at some other wavelength as that of Hawking-Unruh radiation discussed later.

An example of the similarities related to the wake behind an object moving through an external Chameleon (density) field (*i.e.*, atmosphere) is shown in Figure 8, where aircrafts are shown breaking the sound barrier. As shown in Figures 8a, 8b and 8d, the shock patterns are distinctively behind the moving aircrafts, in similar to the vortex field in Figure 6. Noting that, the patterns are respectively larger than that illustrated in Figure 6 due to the denser external field. Also of note, Figure 8c shows the shock pattern a sonic aircraft, where the outward indentation in the shock pattern represents the field expansion and the aft side indentation toward the exhaust represents the field compression, similar to that in Figure 5. Further, by drawing lines perpendicular to the shock lines, one could trace out the Chameleon field lines similar to those about the spaceship in Figure 6. Finally, Figure 8d shows the existence of vortex formation in the aft field.

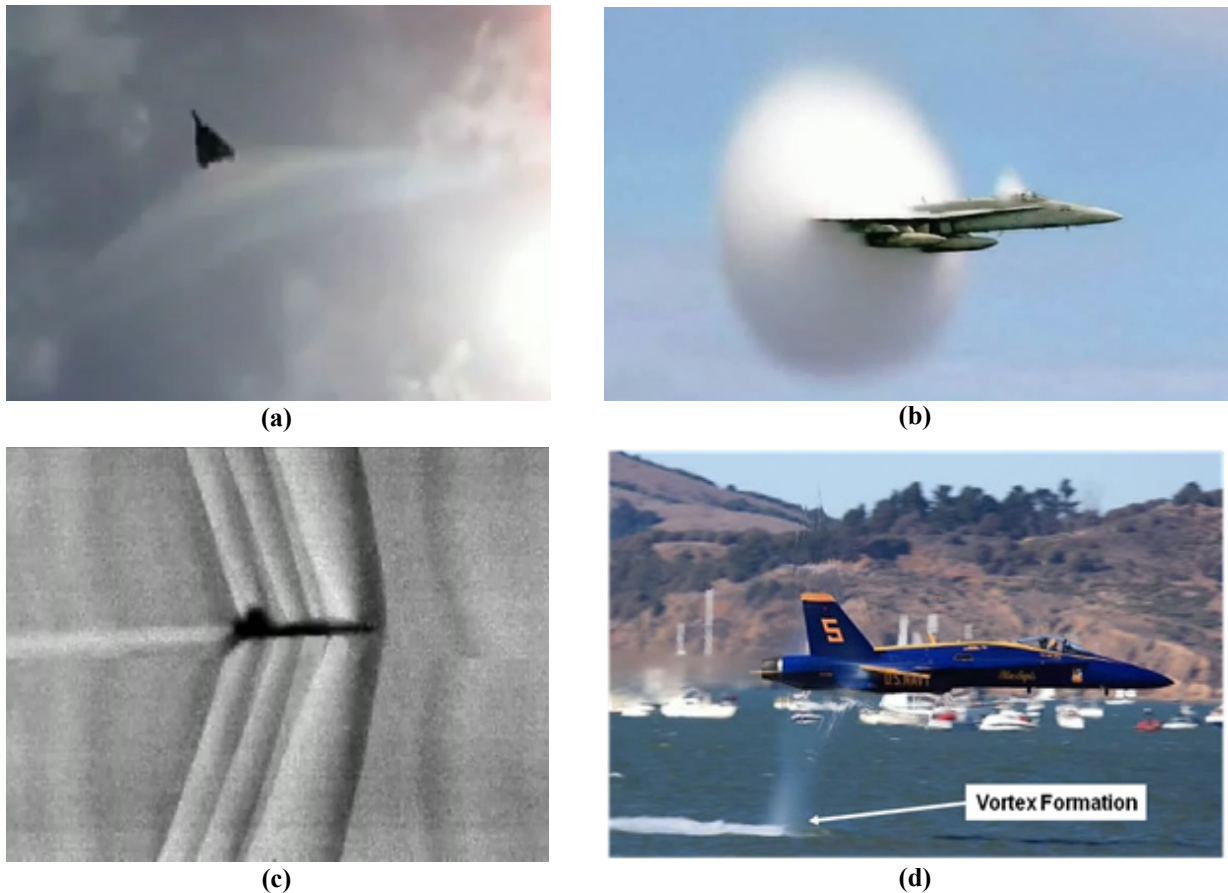


Figure 8. Similarities to Conventional Atmospheric Shock Formations

WARP-DRIVE AND WORMHOLE ANALOGIES

The annular vortex field in Figure 6 formed aft of the spacecraft and its similarity to natural vortex structure as shown in Figure 2 present characteristics to both the Alcubierre Warp Bubble and Wormholes. These characteristic similarities are discussed in the following. Noting that, the authors *do not claim faster than light* in the Modified Chameleon Model, only that there is a resemblance.

Warp-Drive

From the standpoint of spacetime, where in Figure 5 the gravitational expansion forward the spaceship represents a gravity well (Contraction) and the gravitational compression of the thin shell aft of the spaceship represents a gravity

hill (Expansion), the gravitational coupling of the external Chameleon fields have a resemblance to the Alcubierre Warp Bubble as shown in Figure 9. Noting that, for all practical purposes, the Alcubierre Warp Bubble laid down the preliminary ground work toward an active space drive within Einstein Physics, *i.e.*, spacetime.

This resemblance should not be surprising as the Chameleon Model (2004a; 2004b) is also based on Einstein Physics, but carries over to Quantum Field Theory within dark matter/energy models. Where dark matter/energy provides the source of exotic mass/energy required in WarpDrive Models.

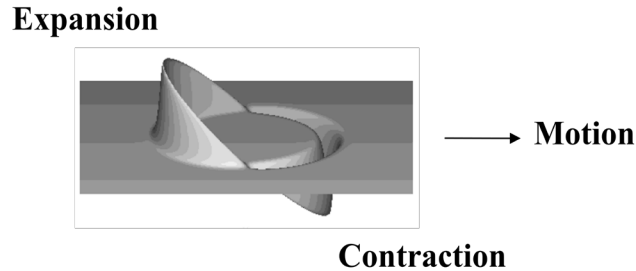


Figure 8. Alcubierre Warp Bubble.

Wormhole

In physics and fiction, a wormhole is a hypothetical topological feature of space time that would be, fundamentally, a "shortcut" through space time. Although wormholes are very popular in science fiction, there is no observational evidence. Although wormholes are valid solutions in general relativity, this is only true if exotic matter can be used to stabilize them. Even if the wormhole is stabilized, it is believed that the slightest fluctuation in space would collapse it. Plus Wormholes allowed by current physical theories might arise spontaneously, but would vanish nearly instantaneously, and would likely be undetectable.

Figure 10 is an artist's impression of a wormhole from an observer's perspective, crossing the event horizon of a Schwarzschild wormhole, which is similar to a Schwarzschild black hole, but with the singularity replaced, by an unstable path to a white hole, in another universe. The observer originates from the right, and another universe becomes visible in the center of the wormhole's shadow once the horizon is crossed; however, this new region is unreachable in the case of a Schwarzschild wormhole, as the bridge, between the black hole and the white hole, always collapses before the observer has time to cross it.

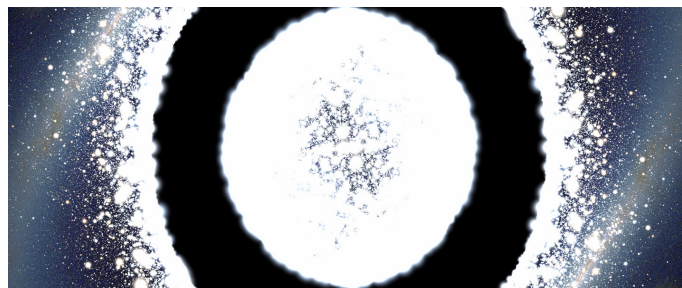


Figure 10. Event Horizon of a Schwarzschild Wormhole

The authors note that the wormhole of Figure 9 has similarities to the aft view of Figure 6. These similarities are shown in Figure 11. As portrayed, the outer wormhole ring represents the annular Vortex field, the white distortion

of space represents the externally modulated Chameleon field, and the distorted center of the wormhole represents the area of the radial change ∂R_{aft} .

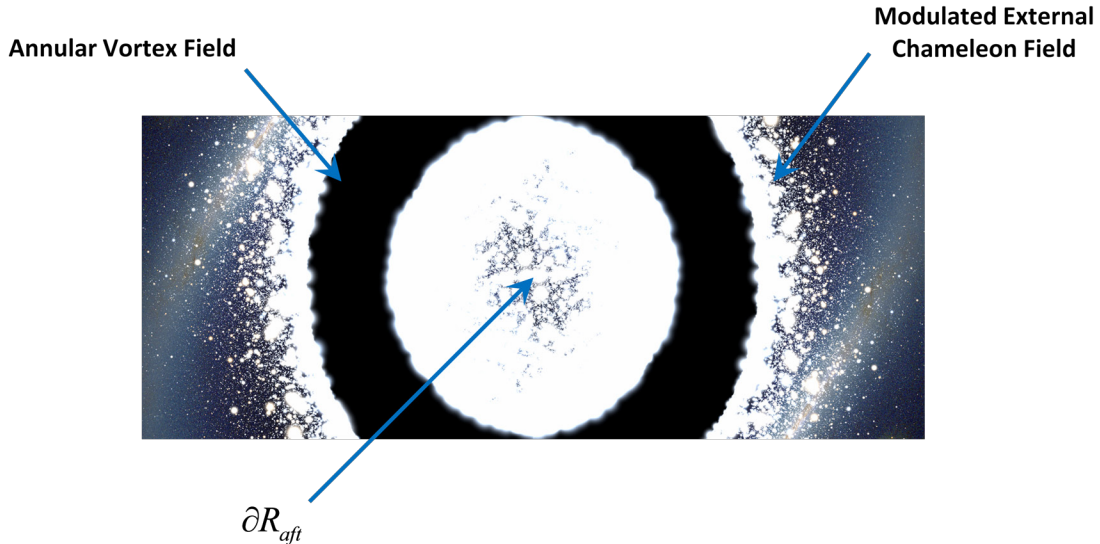


Figure 11. Aft View of a Spaceship Traveling through the Universe Chameleon Field at Light Speed

Hawking-Unruh Radiation

The aft view of Figure 11 implies the emission of black hole or Hawking-Unruh radiation, a measure of the quantum fluctuations in the radiation of accelerated charges from the aft of the spaceship. Noting that, the difference between Hawking and Unruh radiation helps to clarify aspects of the equivalence between radiation in uniform acceleration and in a uniform gravitational field.

According to Hawking (1974), an observer outside a black hole experiences a bath of thermal radiation of temperature

$$T_H = \frac{g}{2\pi k} \left(\frac{\hbar}{c} \right) \quad (20)$$

where g is the local acceleration due to gravity, c is the speed of light, \hbar is Planck's constant and k [1.3806503x10⁻²³ m²kg/s² °K] is Boltzmann's constant. Such that, Hawking radiation in some manner suggests that the background gravitational field interacts with the quantum fluctuations of the electromagnetic field with the result that energy can be transferred to the observer as if he/she were in an oven filled with black-body radiation. Of course, the effect is strong only if the background field is strong. An extreme example is that if the temperature is equivalent to 1 MeV or more, *virtual electron-positron pairs emerge from the vacuum into real particles.*

With respect to Hawking radiation, Unruh (1976) suggested that this phenomenon can be demonstrated in the laboratory according to the principle of equivalence: an accelerated observer in a gravity-free environment experiences the same physics (locally) as an observer at rest in a gravitational field. Therefore, an accelerated observer (in zero gravity) should find him(her)self in a thermal bath of radiation characterized by temperature

$$T_U = \frac{a}{2\pi k} \left(\frac{\hbar}{c} \right) \quad (21)$$

where a is the acceleration as measured in the observer's instantaneous rest frame.

Hawking-Unruh Propulsion

With respect to this paper, the difference in the Hawking and Unruh radiation infers that for a spaceship far from other objects with acceleration a_s and self gravity attraction g_s , that

$$\frac{a_s}{g_s} = \frac{T_U}{T_H}. \quad (22)$$

Whereby, the thrust on the spaceship arises from the difference in the forward Unruh radiation and the aft Hawking radiation, which is given by

$$Thrust = m_s a_s = m_s \left(\frac{T_U}{T_H} \right) g_s, \quad (23)$$

That is, by changing the natural thermal Hawking radiation T_H to Unruh radiation T_U about an object, you can make it move. This is illustrated in Figures 5 and 6, where the gravitational compression of the thin shell produces a temperature change in the region of the radial change ∂R_{eff} corresponding to the Unruh radiation of equation (19).

Such that, *virtual electron-positron pairs*, absorbed by the gravitational expansion forward of the spaceship emerge from the annular vortex field *as real particles*. From this prospective, these real particles are exhausted as normal mass and provide the same thrust mechanism as in normal rocket propulsion.

CONCLUSION

A vortex formation in nature leads to natural propulsive methods. These are seen both at the cosmological scale in such things as blazars and black holes that eject matter to great astrological distances and at the terrestrial level in birds and fishes to propel the environmental fluids (mass) about them. In the Chameleon vortex theory presented in this paper, it is shown that vortex structure behind an accelerating spaceship acquires wormhole like similarities with an overall Warp-Drive appearance. These characteristics provide a method where differences in Hawking and Unruh radiation provides the propulsive method for space travel where *virtual electron-positron pairs*, absorbed by the gravitational expansion forward of the spaceship emerge from the annular vortex field aft of the spaceship *as real particles*, in-like to propellant mass ejection in conventional rocket theory.

REFERENCES

- Birkeland, K., *The Norwegian Aurora Polaris Expedition 1902-1903*, H. Aschehoug & Co, Leipzig, (1908).
- Brax, P., van de Bruck, Carsten, Davis, Anne-Christine, Khoury, Justin and Weltman, Amanda, "Detecting dark energy in orbit: The cosmological chameleon," *Phys. Rev. D*, **70**, (2004a), p. 123518.
- Brax, P., van de Bruck C., Davis A.C., Khoury J. and Weltman A., "Chameleon Dark Energy," in *Phi in the Sky: The Quest for Cosmological Scalar Fields*, AIP Conference Proceedings **P736**, (2004b), pp. 105-110.
- Brito, H. H., "Experimental status of thrusting by electromagnetic inertia manipulation," *Acta Astronautica*, **54**, (2004), pp. 547-558.
- Burnham, S. W., "Note on Hind's Variable Nebula in Taurus," *Monthly Notices of the Royal Astronomical Society*, **51**, (1890), pp. 94-95.
- Cabrit, S., "Jets from Young stars," *Lect. Notes Phys.*, **723**, (2007), pp. 21-53.
- Carlqvist, P., "Cosmic electric currents and the generalized Bennett relation," *Astrophys. Space Sci.* **144**, (1988), pp. 73-84.
- Dickinson, M., "Animal Locomotion: How to walk on water," *Nature*, **424**, (2003), pp. 621-622.
- Feigel, A., "Quantum Vacuum Contribution to the Momentum of Dielectric Media," *Phys. Rev. Lett.*, **92**(2), (2004), p. 020404-1.
- Hartigan, P., Edwards, S. and Pierson, R., *Infrared Emission Lines of [Fe II] as Diagnostics of Shocked Gas in Stellar Jets*, *Ap. J.*, **614** (2004), p. L69.
- Hawking, S. W., "Black Hole Explosions," *Nature* 248, 30-31 (1974)
- Khoury, J. and Weltman, A., "Chameleon cosmology," *Phys. Rev. D*, **69**, (2004a), p. 044026.
- Khoury, J. and Weltman, A., "Chameleon Fields: Awaiting Surprises for Tests of Gravity in Space," *Phys. Rev. Lett.*, **93**, (2004b), p. 171104.

- Kronenberg, P. P., Dufton, Q. W., Li, H., and Colgate, S. A., "Magnetic energy of the intergalactic medium from galactic black holes," *Astrophys. J.*, 560, (2001), pp. 178-186.
- Linden, P. F. and Turner, J. S., "Optimal vortex rings and aquatic propulsion mechanisms," *Proc. R. Soc. Lond. B*, **271**, (2004), pp. 647-653.
- Marscher, A. P. *et al.*, "The inner jet of an active galactic nucleus as revealed by a radio-to- γ -ray outburst," *Nature*, **452**, (2008), pp. 966-969.
- Pinheiro, Mario J., "Electromagnetotoroid Structures in Propulsion and Astrophysics," in the proceedings of *Space, Propulsion & Energy Sciences International Forum (SPESIF-10)*, edited by Glen A. Robertson, AIP Conference Proceedings **1208**, Melville, New York, (2010).
- Potemra, T. A., "Observation of Birkeland Currents with the TRIAD Satellite," *Astrophysics and Space Science*, **58**(1), (1978), pp. 207-226.
- Priest, E. and Forbes, T., *Magnetic Reconnection*, Cambridge University Press, Cambridge, (2000), p.442.
- Robertson, Glen A., "Engineering Dynamics of a Scalar Universe, Part I: Theory & Static Density Models," Lecture Series paper in the proceeding of *Space, Propulsion & Energy Sciences International Forum*, edited by Glen A. Robertson, AIP Conference Proceedings **1103**, Melville, New York, (2009a).
- Robertson, Glen A., "Engineering Dynamics of a Scalar Universe, Part II: Time-Varying Density Model & Propulsion," Lecture Series paper in the proceedings of *Space, Propulsion & Energy Sciences International Forum (SPESIF-09)*, edited by Glen A. Robertson, AIP Conference Proceedings **1103**, Melville, New York, (2009b).
- Robertson, Glen A., "The Chameleon Solid Rocket Propulsion Model," in the proceedings of *Space, Propulsion & Energy Sciences International Forum (SPESIF-10)*, edited by Glen A. Robertson, AIP Conference Proceedings **1208**, Melville, New York, (2010).
- Shawyer, Roger, "Microwave Propulsion – Progress in the EMDrive Programme," in the proceedings of the International Astronautical Congress, IAC08-C4.4.7, (2008).
- Unruh, W. G., "Notes on Black Hole Evaporation," *Phys. Rev. D* 14, 870-892 (1976),
- Woodward, James F., "Investigation of Propulsive Aspects of Mach Effects," in the proceedings of the *Space, Propulsion and Energy Sciences International Forum (SPESIF-09)*, edited by G. A. Robertson, AIP Conference Proceedings **1208**, Melville, New York, (2009).
- Woodward, James F., "A Test for the Existence of Mach Effects With a Rotary Device," in the proceedings of *Space, Propulsion & Energy Sciences International Forum (SPESIF-10)*, edited by Glen A. Robertson, AIP Conference Proceedings **1208**, Melville, New York, (2010).